Journal of Sound and Vibration (1997) **208**(5), 803–822

THE AEROACOUSTICS AND AERODYNAMICS OF HIGH-SPEED COANDA DEVICES, PART 2: EFFECTS OF MODIFICATIONS FOR FLOW CONTROL AND NOISE REDUCTION

P. W. CARPENTER

Department of Engineering, University of Warwick, Coventry, CV4 7AL, England

AND

C. SMITH

School of Mathematics and Statistics, University of Plymouth, PL4 8AA, England

(*Received* 23 *January* 1996, *and in final form* 14 *July* 1997)

The paper describes two studies of the effects of flow control devices on the aerodynamics and aeroacoustics of a high-speed Coanda flow that is formed when a supersonic jet issues from a radial nozzle and adheres to a tulip-shaped body of revolution. Shadowgraphy and other flow-visualization techniques are used to reveal the various features of the complex flow fields. The acoustic characteristics are obtained from far- and near-field measurements with an array of microphones in an anechoic chamber. First the effects of incorporating a step between the annular exit slot and the Coanda surface are investigated. The step is incorporated to ensure that the breakaway pressure is raised to a level well above the maximum operating pressure. It substantially increases the complexity of the flow field and acoustic characteristics. In particular, it promotes the generation of two groups of discrete tones. A theoretical model based on a self-generated feedback loop is proposed to explain how these tones are generated. The second study investigates the effects of replacing the annular exit slot with a saw-toothed one with the aim of eliminating the discrete tones and thereby substantially reducing the level of noise generated.

1. INTRODUCTION

The Coanda effect is exploited in a wide, if somewhat miscellaneous, range of engineering applications.† In the aerospace industry these include circulation-control wings, upper-surface blowing and thrust vectoring. Substantial flow deflection is a central feature of these devices. Thus they make direct use of the Coanda effect. Most of the high-speed, high-pressure, non-aeronautical industrial applications exploit another characteristic of Coanda flows, namely the enhanced turbulence levels and entrainment compared with conventional jet flows. Various burners and combustors are based on this principle. The waste gas flares described by Desty *et al*. [2–4] are good examples. These include two types of external Coanda waste gas flare: the Indair, which has an axisymmetric tulip-shaped Coanda surface with the gas issuing from an annular exit slot located at the base of the tulip; and the Stedair, a steam-assisted flare. The Indair is of particular significance in the present context, because the present work was carried out as part of a research programme on its aeroacoustics and aerodynamics.

† The literature on high-speed Coanda flow and its applications is reviewed in reference [1].

0022–460X/97/500803 + 20 $25.00/0/sv971203

The inventor of a Coanda device is faced with two important problems when attempting to refine the design in order to maximize the enhanced entrainment. Firstly, if the curvature of the Coanda surface is too great and/or the operating pressure too high, the flow will break away completely from the surface. This could have catastrophic consequences for a burner or combustor. The second problem concerns the aerodynamic noise generated by the device. This is much less serious because Coanda devices often generate less noise than their conventional counterparts [3–5]. In practice the two problems can be inter-related. For example, in the case of the Indair waste gas flare, a step is incorporated between the exit slot and the Coanda surface (see Figures 1 and 2) in order to eliminate any possibility of breakaway occurring within the range of operating pressures. But the presence of this step substantially increases the level of noise generated; at least, it does in model experiments [6]. It is the effect of the step on the aeroacoustics which forms the first main section of the present paper.

Although the noise generated by Coanda devices may be less than those of comparable conventional ones, the enhanced turbulence levels and complex shock wave patterns usually make noise reduction desirable, if not essential. The second main section of the paper gives an account of an experimental study of a noise-reducing device. This device simply involves replacing the annular exit slot with a "toothed" exit slot. Such a device cannot be used, of course, if it has an unacceptably adverse effect on breakaway. So, once again, there is an interplay between the requirements for preventing breakaway and reducing noise.

2. EFFECTS OF A STEP ON THE FLOW FIELD AND AEROACOUSTICS

Except where explicitly noted, the experimental set-up and procedures are identical to those of reference [1]. A fairly comprehensive investigation of the effects of a step on the

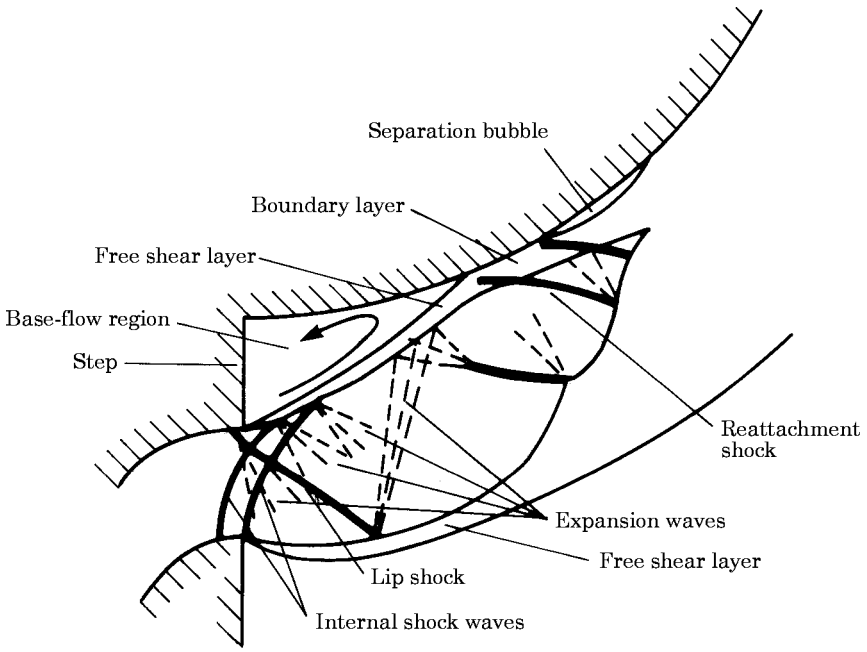

Figure 1. Schematic sketch of the key features of the flow field for a model Indair with a step.

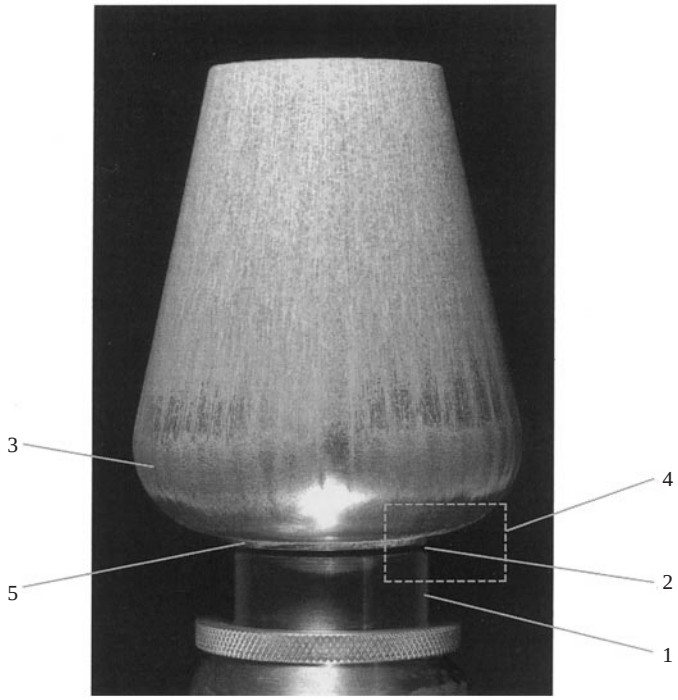

Figure 2. A photograph of the Coanda model fitted with a 2 mm step and with the exit-slot width adjusted to configuration C of Table 1. The figure also shows a surface oil-film visualization carried out at a stagnation pressure ratio $p_0/p_\infty = 5{\cdot}2$. Key: 1, adjustable sleeve for varying slot width; 2, annular exit slot; 3, Coanda surface; 4, region corresponding to shadowgraph photographs in Figures 3(a) and 3(b); 5, step between exit slot and Coanda surface.

flow field and aeroacoustics has been given by Parsons [6]. Here one concentrates only on those aspects of the study which are considered to be of general interest.

2.1. THE FLOW FIELD

The experimental set-up used to investigate the effects of the step on the flow field and aeroacoustics of the high-speed Coanda flow was described in reference [1].

The device used for the experiment was a 1/8th scale model of a 33 in diameter Indair flare† with air replacing waste gas as the working fluid for the model tests. The model comprised a "tulip-shaped" body of revolution with an annular nozzle leading to an exit slot located at the base of the tulip. For the study described here the model was fitted with a standard step of 2 mm height which corresponds to the Indair 33. In all other respects the geometry is the same as that detailed in reference [1]. A photograph of the model with a fixed step is shown in Figure 2 which also shows a surface oil-film flow visualization. It is included at this point to depict the form of the Coanda model. A version of Table 1 from reference [1], giving the exit-slot configurations used, is reproduced below; an additional fifth exit-slot configuration is included here.

Some results from reference [7] which were obtained with a similar model fitted with an adjustable step are also presented. The effect on the flow field of installing a step between the exit slot and the Coanda surface is shown schematically in Figure 1. Comparison with Figure 2 of reference [1] makes it immediately apparent that the flow

† The Indair waste-gas flare is designed and marketed by Kaldair Ltd.

field near the nozzle exit is very different. Figure 1 is based on a series of shadowgraph photographs. Examples are given in Figure 3. These were made for a range of operating pressures. As can be seen the quality of the shadowgraph is not good. The axisymmetric flow geometry seems to be the major cause of the problems. Shadowgraphy was used instead of schlieren photography because the authors wished to obtain flow visualizations with a video camera and monitor simultaneously with acoustic measurements. The suspended floor of the anechoic chamber was so flexible that it was very difficult to make the necessary fine adjustments to the schlieren system. The flow-visualization study was therefore confined to the less sensitive shadowgraph technique. It was, in fact, very useful for discovering some of the details of the flow field to have instantaneous video output which allowed one to observe small changes in the flow field as the operating pressure was changed. One could also observe the changes in the flow field that accompanied significant changes in the character of the acoustic signal measurements. It should be made clear, however, that the flow-visualization apparatus was removed for making the sound measurements described below in section 2.2 and thereafter.

The most prominent feature of the flow field in Figure 1 is the base-flow region (also labelled 4 in Figure 3) behind the step. This is similar to the flow field revealed in the classic studies of Chapman [8] and Korst [9] for supersonic flow over a rearward-facing step or blunt-based trailing edge. An essential feature is the relatively low pressure recirculating flow in the base region. A free shear layer forms along the interface between the supersonic flow issuing from the exit slot and the recirculating base flow. This free shear layer reattaches to the surface and recompression occurs through a reattachment shock wave which forms to accommodate the required change of direction. Another feature of base flows is the lip shock wave. In the classic base flow downstream of a rearward-facing step the lip shock assumes a direction which is almost parallel to the free shear layer. Here this is certainly not so, leaving some doubt as to whether the feature labelled 6 in Figure 3(b) is correctly identified both there and in Figure 1. Note that the lip shock which appears in the flow fields described in reference [1] emanates from the lower edge of the exit slot (at the top of the adjustable sleeve), whereas in the present case the lip shock emanates from the upper edge of the exit slot at the step, as in classic base flow. The internal shock waves (labelled 8 in Figure 3(b)) reflect from the inner shear layer as expansion waves whereas in the absence of the step they would reflect from the solid surface as shock waves. So in these ways the presence of the step tends to weaken the shock-wave pattern near the exit slot. The absence of the lip shock emanating from the lower edge of the exit slot, which is found with the stepless Coanda model, is particularly significant since it appeared in reference [1] to generate a separation bubble when it was incident on the Coanda surface. And it was this separation bubble that grew in size and ultimately caused breakaway to occur.

TABLE 1

Dimensions of exit slots. R_C is the radius of curvature of the Coanda surface profile near the exit slot

Slot	Slot-width b (mm)	b/R_C
A	0·625	0·025
B	1·25	0·05
C	1·875	0·075
D	2·5	0·1
E	3·125	0·125

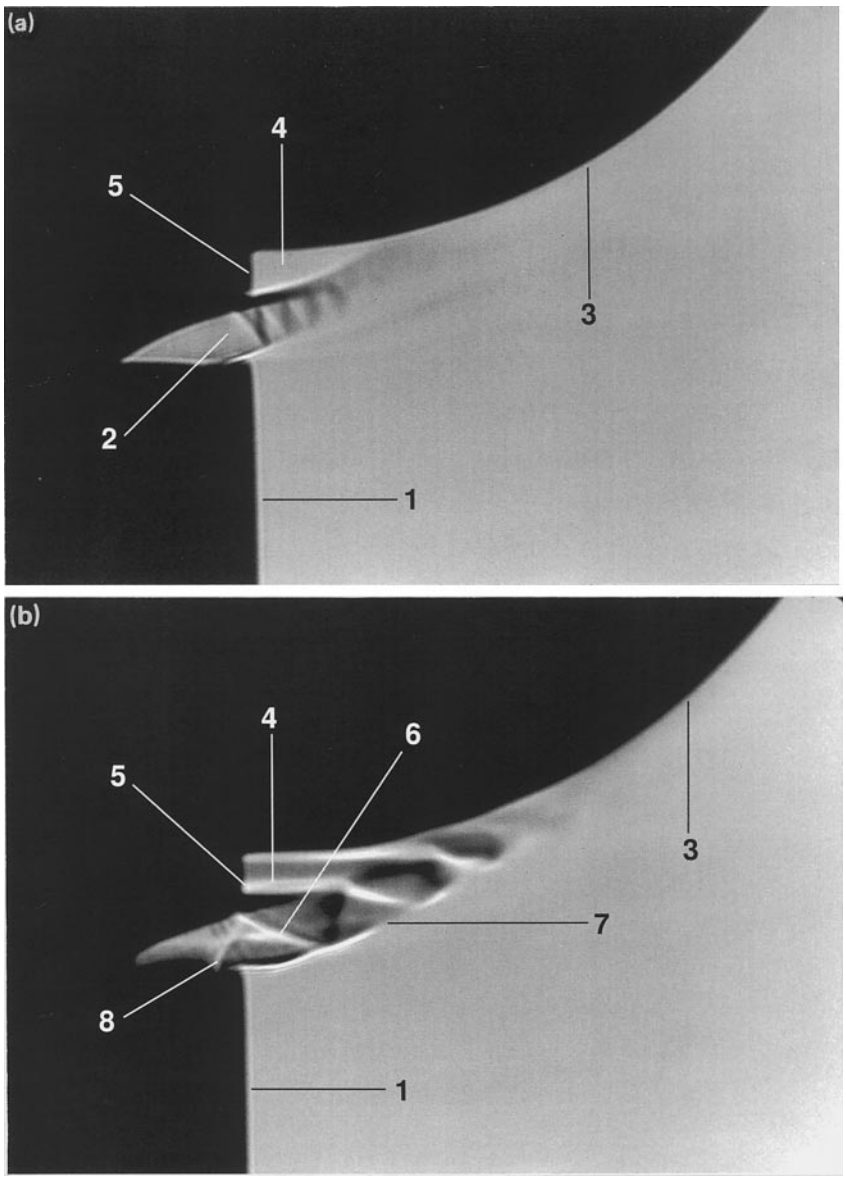

Figure 3. Shadowgraphs of the flow field corresponding to region 4 in Figure 2 near the nozzle exit for slot C with a 2 mm step. (a) $p_0/p_\infty = 2{\cdot}03$; (b) $p_0/p_\infty = 4{\cdot}45$. Key: 1, adjustable sleeve; 2, annular exit slot; 3, Coanda surface; 4, base-flow region downstream of the step; 5, step between exit slot and Coanda surface; 6, possible lip shock; 7, jet boundary; 8, internally generated shock wave.

It has been firmly established in a recent study by Gregory-Smith and Senior [10] that fitting a step does indeed postpone breakaway to a higher operating pressure. Their experimental study was carried out for both two-dimensional and axisymmetric high-speed Indair-type Coanda flows. The external geometries of their models are very similar to that used for the present study, but the internal geometry of their models is significantly different. Whereas the present model replicates the internal nozzle shape of the Indair flare their nozzle contour is specially designed to avoid internal disturbances, so the internal shock waves depicted in Figure 1 were either absent or much weaker. The simple

explanation for how the step acts to postpone breakaway to higher pressures relies on the enhanced pressure difference between the ambient air and the low pressure base flow. This may well be part of the explanation, but for high-speed flow shock wave–boundary layer interaction seems to be an important factor in the absence of the step. Gregory-Smith and Senior [10] suggested that the step makes the shock structure more complex resulting in the formation of smaller but more numerous separation bubbles. Their results suggest that the second and third bubbles on their model amalgamate before the first bubble can join them to cause breakaway. Our study suggests that one of the effects of the step is to eliminate the lip shock emanating from the lower edge of the exit slot. For the unstepped models [1] this shock appeared to be responsible for forming the first separation bubble when it intersects the Coanda surface. Thus with the present stepped models the first bubble forms further round the surface and is much smaller. The shock pattern also appears to be more complex and somewhat weaker. However, any conflict between the present interpretation and that of Gregory-Smith and Senior [10] may be more apparent than real.

2.2. SOUND PRESSURE LEVELS

The sound pressure level is plotted in Figure 4 as a function of angle relative to the horizon for slot A of Table 1 at four different values of the pressure ratio, p_0/p_∞ (where p_0 and p_∞ are the stagnation and ambient pressures respectively). Figure 5 of reference [1] shows the orientation of the model, negative angles correspond to directions below the horizon. Figure 4 can be compared directly to Figure 10 of reference [1] which corresponds to a stepless configuration, but which is otherwise identical. Plainly the step causes a steep rise in the maximum sound pressure level and also has a very marked effect on the directivity pattern. The rather irregular directivity pattern at $p_0/p_\infty = 2{\cdot}4$ is caused by the generation of discrete tones. At the other pressure ratios the step shifts the direction of maximum sound pressure level to well below the horizontal for this particular configuration. This did not always occur for other configurations of exit slot. It can usually

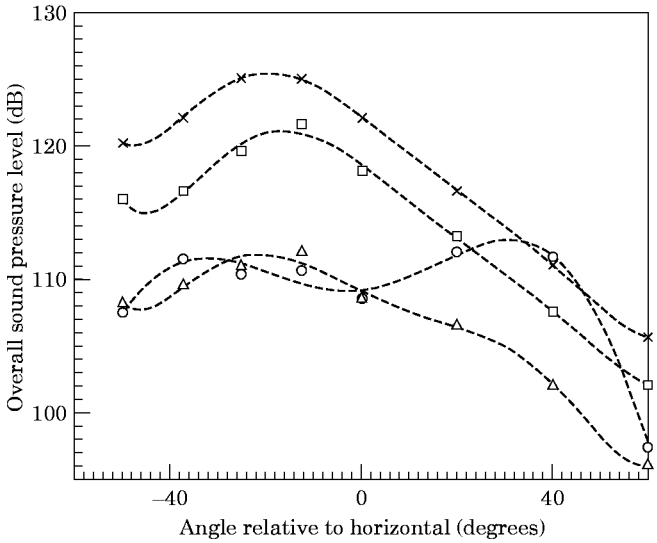

Figure 4. Directivity of the overall sound pressure level for slot A with a 2 mm step. The values of p_0/p_∞ are as follows: --○--, 2·4; --△--, 3·8; --□--, 5·2; -- × --, 6·6.

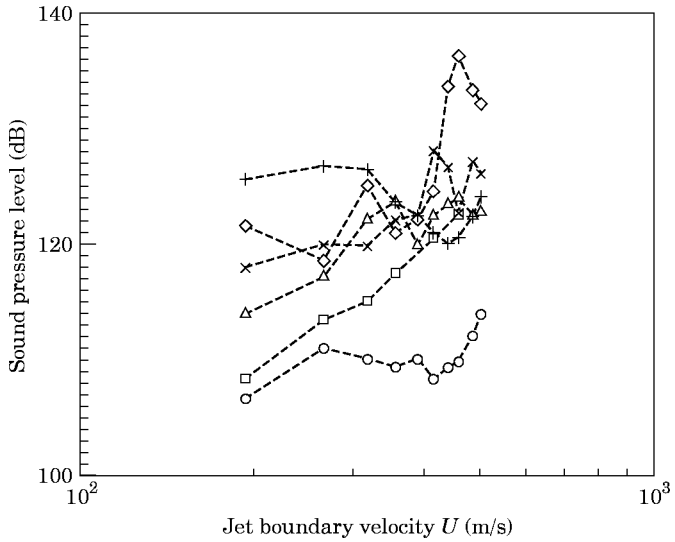

Figure 5. Sound pressure level versus jet boundary velocity, U, for various slot widths with a 2 mm step. --○--, slot A; --△--, slot B; -- × --, slot C; --◇--, slot D; -- + --, slot E; --□--, saw-toothed exit slot with slot C.

be safely assumed that installing a step will lead to a considerable rise in sound pressure level, but there are no clear trends as regards directivity.

The variation of the *SPL* radiated in the horizontal direction with the flow speed, U, on the jet boundary at the nozzle exit is plotted in Figure 5 for all five slot widths given in Table 1. This figure may be directly compared with Figure 11 of reference [1] where the data are plotted from the corresponding stepless configurations. In Figure 11 of reference [1] the data mostly followed fairly closely the well-known U^8 variation found with round jets. With the stepped models no clear trend can be discerned in Figure 5. Again this is because of the generation of discrete tones.

The effect of the step is, perhaps, shown most dramatically by Figure 6. These results were obtained by plotting the r.m.s. value of the microphone amplifier output against the output voltage of the pressure transducer while slowly increasing the stagnation pressure. It can be seen in Figure 6(a) that for the stepless configuration there is a monotonic rise

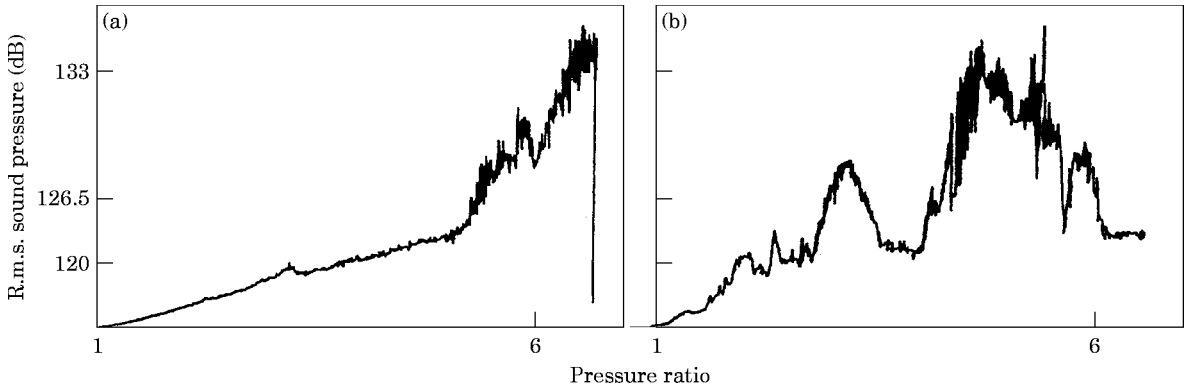

Figure 6. R.m.s. sound pressure level plotted against pressure ratio. (a) Slot C without a step; (b) slot C with a 2 mm step.

in *SPL* as the stagnation pressure is increased, whereas for the stepped configuration a range of stagnation pressures with relatively high *SPL* may be followed by a range of higher pressures with much lower values of *SPL*. This behaviour is explained by the fact that discrete tones are generated for most of the operating range of pressures, but for isolated bands of stagnation pressure they cease to be generated or the directivity pattern changes suddenly for no apparent reason. The other point to note is that in Figure 6(a) a very steep drop in *SPL* occurs at a pressure slightly above 6·6 bar. This indicates that breakaway has occurred. This does not occur in Figure 6(b), confirming that the presence of the step has postponed breakaway to a higher stagnation pressure.

2.3. SPECTRA AND DISCRETE TONES

The spectra for the present stepped configuration were acquired only in the frequency domain by using a Hewlett Packard 3582A spectrum analyzer, whereas in reference [1] the spectra were computed from the time domain into the frequency domain by using an FFT processing routine. Otherwise the experimental set-up was as described in reference [1].

Typical power spectra for the slot C configuration with the standard step are plotted in Figure 7 for various stagnation pressures. It is immediately apparent that discrete tones were generated throughout the pressure range. In this case the microphone was located at 12·5° below the horizontal, but the amplitudes of the discrete tones did not vary greatly with direction. As indicated by Figure 6(b) discrete tones were not generated continuously throughout the range of stagnation pressures. They tend to disappear abruptly at certain stagnation pressures to reappear again at a slightly higher pressure. The underlying broadband noise peaks at very similar frequencies to the unstepped case. This is apparent in the spectra reported in reference [6] for low stagnation pressures. Thus the broadband turbulent mixing noise is probably not greatly affected by the presence of a step and follows the scaling laws suggested in reference [1].

Figures 8 and 9 (based on similar figures in reference [7]) show how the dominant frequencies of the discrete tones vary with, respectively, exit-slot width keeping step height fixed and step height keeping the exit-slot width fixed. In most cases there are higher harmonics and sometimes lower harmonics. In both Figures 8 and 9 several sets of data can be discerned as suggested by the regions surrounded by broken-line curves. These sets of data can be divided into two groups. Group A occurs at relatively low pressures and is characterized by a tendency for frequency to be almost invariant with stagnation pressure for a particular configuration. In contrast group B, which occurs at relatively high stagnation pressures, appears to consist of two or three separate stages within which the frequency falls steeply with a rise in pressure. In Figure 8 in the case of the smallest exit-slot width of 1·25 mm, three distinct stages of the group B discrete tones can be discerned, each characterized by a sharp jump to a higher frequency followed by a steep drop in frequency with a further rise in stagnation pressure; whereas in Figure 9 there is only a hint of a second stage at the highest pressure.

The group B discrete tones are undoubtedly a manifestation of those found at high stagnation pressures in reference [1]. It can be seen that the data from the stepless model plotted in Figure 8 fall within the same band of data points as for the stepped case. In reference [1] it was suggested that these high-pressure tones were generated by a self-excited feedback mechanism involving the separation bubbles. It appears from Figure 9 that the group B discrete tones are not greatly affected by the step height and from Figure 8 it appears as if the main effect of exit-slot width is to determine the pressure at which the transition from group A to group B and the jumps to higher stages occur.

For the group A tones the frequency does not vary greatly with stagnation pressure. No clear trend with slot width is apparent in Figure 8. From Figure 9, however, a clear

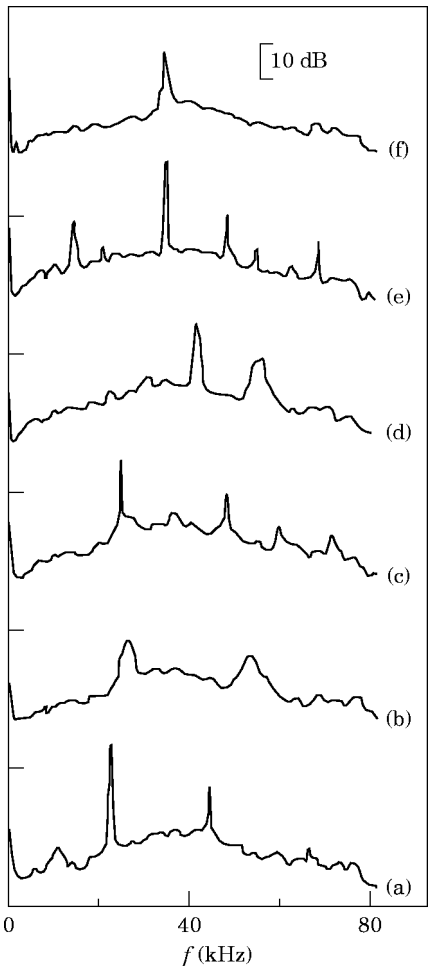

Figure 7. Power spectra at various pressure ratios for slot C with a 2 mm step. The microphone was located at 12·5° below the horizontal direction. The bandwidth was 30 Hz. The values of p_0/p_∞ are as follows: (a) 2·025; (b) 2·8; (c) 3·25; (d) 4·25; (e) 5·125; (f) 5·675.

trend does appear; the frequency tends to fall as the step height is increased. The data point for the 2 mm step in Figure 9 can probably be ignored for this purpose since it corresponds to the model used to obtain the data plotted in Figure 8, whereas the remaining data in Figure 9 correspond to a model with an adjustable step; and the adjustable-step model had a slightly different internal nozzle contour.

A theoretical model for explaining the generation of discrete tones in group A is illustrated in Figure 10. The free shear layer, which forms the outer boundary of the base-flow region behind the step, will be unstable to wave-like disturbances. In fact, the coherent structures found in free shear layers bear a close likeness to wave-like Kelvin–Helmholtz instabilities. These will propagate along the shear layer, growing in amplitude. Depending on their phase when the disturbances reach the reattachment zone, the base-flow region will either open to admit fluid from downstream or close, thereby causing fluid to be ejected. If this process of opening and closing occurs in a regular periodic manner it will effectively create an acoustic monopole source at the reattachment point. The monopole would then radiate sound waves back inside the base-flow region to

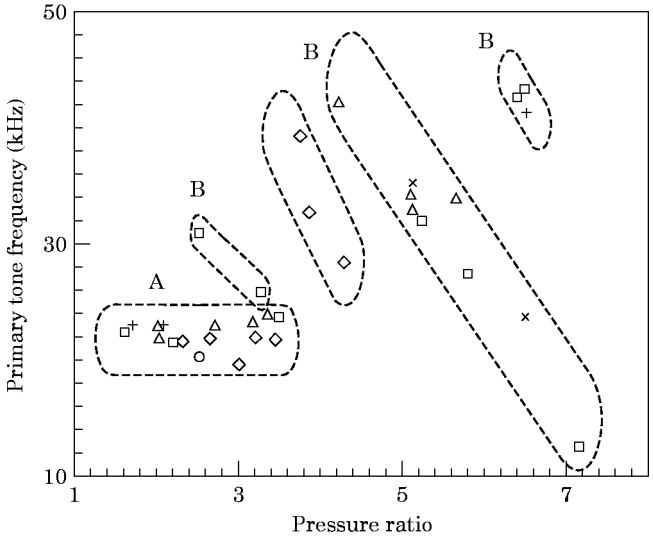

Figure 8. Primary tone frequency versus pressure ratio for various slot widths. Slot widths for stepless surface: +, 1·25 mm; ×, 1·875; slot widths for 2 mm step: ○, 3·125 mm; ◇, 2·5 mm; △, 1·875 mm; □, 1·25 mm.

the exit slot where disturbances would be generated. In this way the basic conditions for a self-sustained acoustic feedback loop can be seen to exist.† In certain respects the proposed mechanism is similar to that formulated by Rossiter [13], Heller *et al*. [14] and Bilanin and Covert [15] for explaining the generation of discrete tones by aerodynamic flows over shallow cavities. The reattachment shock wave (see Figure 1) may well also be caused to oscillate by the inflow–outflow mechanism. A strong oscillating force acting normal to the Coanda surface would thereby be generated. This would contribute an additional or alternative acoustic source at approximately the same location, but would leave the simple theoretical arguments advanced below more or less unchanged.

Three conditions need to be met in order for the feedback loop to function in the base-flow region.

(1) The frequency (in Hz) of the wave-like disturbances generated at the exit slot must be equal to the acoustic frequency within the base-flow region, i.e.,

$$f = c_w / \lambda_w = a_b / \lambda_b, \tag{1}$$

where c_w and λ_w are the phase speed and wavelength of the wave-like disturbances (coherent structures), and a_b and λ_b are the speed of sound and its wavelength within the base-flow region. The estimate of the acoustic frequency given in equation (1) implies that the recirculating flow speed in the base-flow region has a negligible effect. In conventional base flows the recirculating flow tends to occur at fairly low subsonic speeds, so neglecting its effect is probably not a bad assumption.

(2) The phase shift of the disturbance as it travels from the exit slot to the reattachment zone plus the phase shift of the acoustic wave travelling in the reverse direction within the base-flow region must equal $2\pi n$ where n is an integer; i.e.,

$$2\pi L(1/\lambda_w + 1/\lambda_b) = 2\pi(n + \xi), \tag{2}$$

† The role of self-sustained feedback loops in generating tones can be traced back at least as far as the seminal papers of Powell [11, 12].

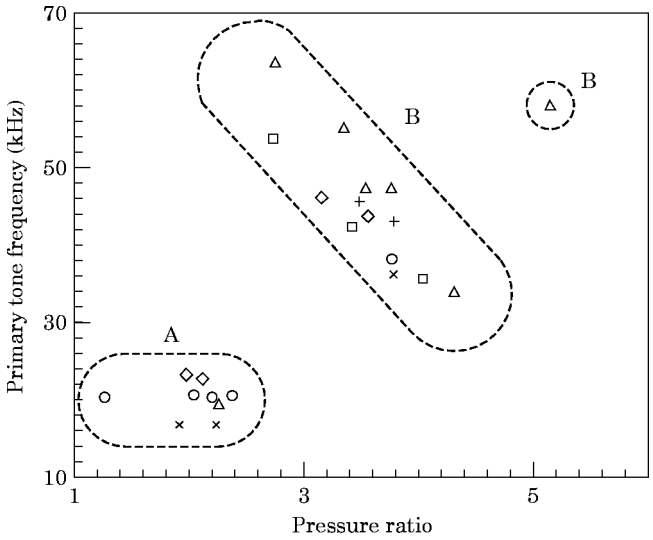

Figure 9. Primary tone frequency versus pressure ratio for slot C with various step heights. Step heights: +, 7·2 mm; ×, 5·9 mm; ○, 4·4 mm; ◇, 3·4 mm; △, 2·0 mm; □, 1·0 mm.

where $L = l_b / \cos\theta_2$, as can be seen from Figure 11, is the approximate length of the undisturbed free shear layer. A correction factor ξ has been introduced in equation (2) to allow for any delays caused by the sound-generation process in the reattachment zone and the process whereby the disturbances are generated by the impingement of sound waves at the exit slot. Heller *et al*. [14] found that, for shallow rectangular cavities up to a Mach number of about 1·5, a value of $\xi = 0{\cdot}25$ gave good agreement with experimental data. By combining equations (1) and (2) it can be shown that the frequency generated is given by

$$fL/U_2 = n + \xi/[(U_2/c_w) + (U_2/a_b)], \tag{3}$$

where U_2 is the flow speed corresponding to the Mach number M_2 along the outer boundary of the base-flow region in Figure 11.

(3) The phase speed c_w must be close to that for the most rapidly growing instability wave or, from a slightly different perspective, close to the so-called convection speed of the coherent structures.

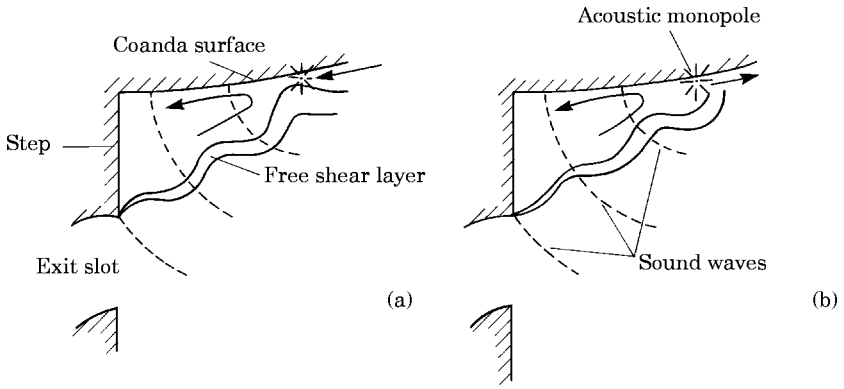

Figure 10. Schematic sketch depicting the mechanism for generating group A discrete tones. (a) Inflow into base-flow region; (b) outflow from base-flow region.

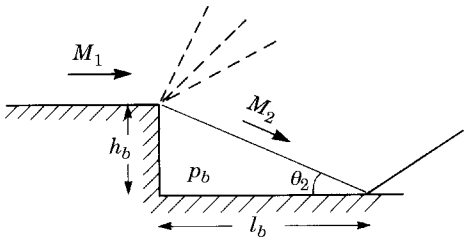

Figure 11. Schematic sketch of a classic supersonic base flow.

In order to use equation (3) to estimate the frequency it is necessary first to make reasonable estimates for L, U_2, a_b and c_b/U_2.

The approximate length, L, of the free shear layer defining the edge of the base-flow region behind the step can be obtained from shadowgraphs like those in Figures 3(a) and (b).

To obtain an estimate of the flow speed, U_2, it should first be noted that the group A tones only appear for pressure ratios ranging from about 1·3 to 3·4. According to the quasi-one-dimensional theory described in reference [1], the internal profile of the annular nozzle leading to the exit slot corresponds to a convergent–divergent nozzle such that the critical pressure ratio for choked flow is about $p_0/p_\infty = 1{\cdot}53$ and the exit pressure becomes equal to the ambient pressure at about $p_0/p_\infty = 2{\cdot}5$. So, it appears that the group A tones are mostly generated when the flow is over-expanded with near-normal shock waves present near the nozzle exit. This view is borne out by the shadowgraph shown in Figure 3(a). Accordingly, for much, if not all, of the range of pressure ratios, the flow along the edge of the shear layer enclosing the cavity behind the step will be close to sonic.

If the flow speed is neglected in the base-flow region it can be assumed to a reasonable approximation that the speed of sound there corresponds to the recovery value, so using isentropic-flow relations gives

$$a_2/a_b = 1/\sqrt{1 + r(\gamma - 1)M_2^2/2}. \tag{4}$$

As noted above, $M_2 = 1$ to a reasonable approximation. For shallow rectangular cavities with Mach numbers in the range 1–1·5 Heller *et al*. [14] found that the recovery factor, $r \approx 0{\cdot}9$, rising to values even closer to 1 at higher Mach numbers. Hence to a good approximation a value $r = 1$ can be assumed in the present context, implying that a_b equals the stagnation speed of sound, which for the experimental conditions in question can be taken to be about 350 m/s.

The extent to which the free shear layer bounding the base-flow region is similar to more conventional high-speed shear layers is rather questionable. Thus it could be argued that $c_w/U_2 = 0{\cdot}5$ is a sufficiently good approximation given all the uncertainty. However, it may be worth further pursuing the analogy between the coherent structures in the shear layer and conventional high-speed Kelvin–Helmholtz instability waves. The convection speed of the coherent structures in a conventional high-speed free shear layer can be determined approximately by means of an isentropic model proposed by Bogdanoff [16] and Papamoschou and Roshko [17]. This prediction is based on the well-known argument that the stagnation point between two structures must be pressure balanced. In the present case, if the flow speed in the base region is regarded as negligible, the convection speed is thereby approximated by

$$U_c = c_w = U_2/[1 + k(a_2/a_b)]. \tag{5}$$

TABLE 2

Comparison of theoretical predictions for cavity-tone frequencies with experimentally observed values of the group A frequencies for slot C with a 2 mm step height

p_0/p_∞	L (mm)	f (kHz) Equation (6) with $n = 1$	f (kHz) Experimental values
2·03	4·8	29·9	20·0, 22·9
2·38	6·4	22·5	None
3·19	6·8	21·25	23·2
3·37	6·8	21·25	23·9

k is a correction factor to allow for non-isentropic effects such as stagnation pressure losses due to shock waves; $k = 1$ for the isentropic model. Papamoschou [18] found experimentally that for a combination of supersonic and subsonic streams k was always less than 1 so that $c_w > (c_w)_{k=1}$. On the other hand for this combination of streams Martens *et al*. [19] found significant departures from the isentropic model, but in one case $k > 1$ and in the other $k < 1$. However, in both cases the measured values of c_w were within 7·5% of the isentropic value. Here the value for c_w corresponding to $k = 1$ in equation (5) will be used. With $r = 1$ and $M_2 = 1$ substituted in equation (4), as suggested above, $a_2/a_b = 0{\cdot}913$. When this value is substituted into equation (5) along with $k = 1$, the estimate $c_w/U_2 = 0{\cdot}52$ is obtained which is close to the *ad hoc* value suggested above.

By using the values suggested above for the various quantities in equation (3), the following estimate is obtained for the cavity-tone frequency (in Hz) for the case of a 2 mm step height:

$$f \simeq (115/L)\,(n + \xi). \tag{6}$$

This approximate theoretical estimate is compared with the experimentally observed frequencies in Table 2.

As can be seen from Table 2 there is a reasonably good agreement between the theoretical and experimental values. Further corroboration for the theoretical model can be found in the way the frequency of the group A tones tends to vary with step height. From the geometry sketched in Figure 11 it can be seen that approximately $L \propto h_b$ and therefore according to equation (6) the frequency will be inversely proportional to step height. It can be seen from Figure 9 that this is roughly what is found for the measured values of frequency, provided the data point corresponding to the 2 mm step height is ignored for the reasons given above. There is little point in making a more precise comparison since the predicted variation of frequency with step height can only be expected to hold in a qualitative sense.

Further evidence for the validity of the proposed model was obtained by carrying out near-field measurements. A Type 4138 1/8 in Brüel and Kjaer (B & K) microphone was traversed in a circular arc of radius 30 mm which kept the microphone at a distance of 5 mm from the Coanda surface. At a pressure ratio $p_0/p_\infty = 2{\cdot}03$, which corresponds to Figure 3(a), the primary frequency was 22 kHz. Accordingly the microphone signal was passed through a tuneable band-pass filter (B & K Type 1621) set at 22 kHz. The filtered and unfiltered signals are both plotted versus angle round the Coanda surface in Figure 12. Note that the filtered microphone signals exhibit a peak at around 17°. The estimates given above, which were in accord with the shadowgraphs, located the reattachment zone at about 6 to 10 mm from the exit slot. This corresponds to about 14° to 23°. Thus there

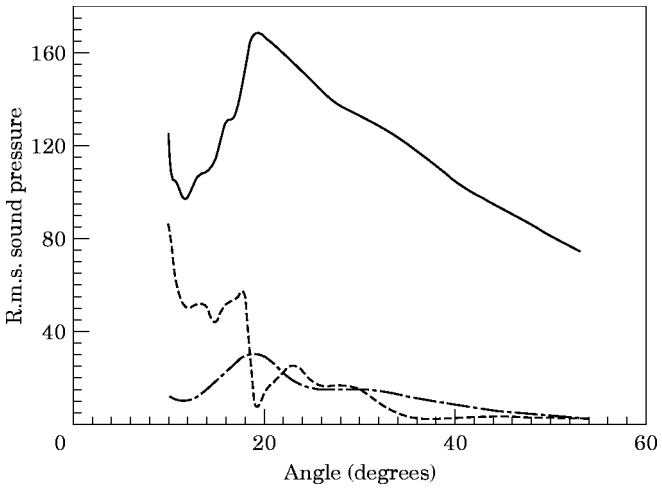

Figure 12. Near-field r.m.s. sound pressure versus angle around the Coanda surface for slot C with 2 mm step. The scale for sound pressure is arbitrary. ——, Unfiltered, $p_0/p_\infty = 2{\cdot}03$; – – –, filtered, $p_0/p_\infty = 2{\cdot}03$; –·–, filtered, $p_0/p_\infty = 2{\cdot}725$.

seems to be fairly firm evidence that the acoustic source responsible for the group A discrete tones is located in the reattachment zone.

3. NOISE SUPPRESSION BY USE OF A SAW-TOOTHED EXIT SLOT

Destroying the coherence of the wave-like large scale structures propagating along the free shear layer bounding the base-flow region behind the step should eliminate the self-sustained acoustic feedback loop described in section 2.3. One way to achieve this is to replace the straight exit slot with a saw-toothed exit slot, as depicted in Figure 13. A photograph of the model with the modified exit slot is shown in Figure 14. Such an exit slot appears to generate strong streamwise vortices which rapidly destroy the axial symmetry of the coherent structures in the mixing-layer region of the Coanda jet near the exit slot. This is shown schematically in Figure 15. The streamwise vortices are evident in the surface oil-film visualization shown in Figure 14 and also in other flow visualizations carried out on models fitted with saw-toothed exit slots [6]. Weaker streamwise vortices appear to be present even when the exit slot is unmodified, as suggested by the surface oil-film visualization shown in Figure 2. They also appear in the case of the unstepped model; see Figure 3 of reference [1]. Comparisons between Figures 14, 2 and Figure 3 of reference [1] suggest that the saw-toothed exit slot promotes the coalescence of smaller

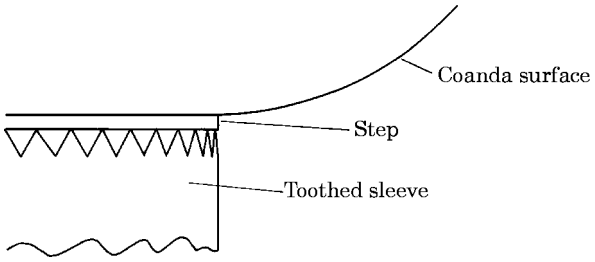

Figure 13. Schematic sketch of the saw-toothed exit slot. The sleeve has a total of 40 teeth. Each triangular tooth has a base measuring 4 mm and a height of 3·6 mm.

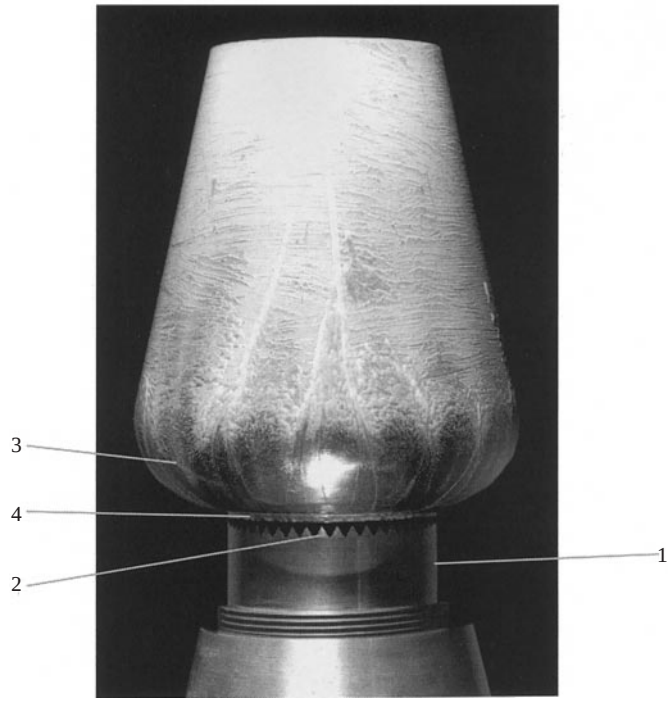

Figure 14. A photograph of the Coanda model fitted with a 2 mm step and a saw-toothed exit-slot width. The figure also shows a surface oil-film visualization carried out at a stagnation pressure $p_0/p_\infty = 5{\cdot}2$. Key: 1, adjustable sleeve for varying slot width; 2, saw-toothed exit slot; 3, Coanda surface; 4, step between exit slot and Coanda surface.

streamwise vortices into fewer stronger vortices. Spark schlieren photographs presented in reference [6], but not included in the present paper, showed that the use of a saw-toothed exit slot also leads to a weakening of the shock structure and to enhanced entrainment in the mixing-layer region near the exit slot. The enhanced entrainment was confirmed by measurements reported in reference [20].

It has been known for some time that the use of tabs can suppress the screech noise generated in conventional supersonic jets [21]. More recently the effects of tabs on the aerodynamics and aeroacoustics of high-speed jets have been studied in some detail by Ahuja *et al*. [22, 23] and Samimy *et al*. [24]. The recent study of Zaman *et al*. [25] is the most relevant to the present work. They investigated the use of delta tabs attached to the exit of an otherwise round nozzle in such a way as to point in the streamwise direction at an angle of 45° to the nozzle axis. Such tabs were found to be more effective in suppressing screech and broadband jet noise than the previously studied rectangular tabs. The similarity between this concept and the saw-toothed exit slot is fairly clear, particularly when one sees the details on the generation of streamwise vortices presented in reference [25].

Zaman *et al*. [25] found that the delta tabs led to gross changes in the overall jet structure. The use of two tabs completely bifurcated the jet, while three or four tabs resulted in the formation of a corresponding number of "fingers" in the mixing layer. In the case of a Coanda flow one needs to approach modification of the jet structure with caution, since it can all too easily destroy the Coanda effect. In fact, the authors experimented with several different modifications of the exit-slot geometry. Apart from the saw-toothed configuration shown in Figures 13 and 14, all but one of the other

modifications destroyed the Coanda effect. The only other modification which suppressed the discrete tones without causing flow breakaway was to cover the exit slot in fine wire gauze. The use of square-toothed exit slots led to a particularly striking effect, somewhat reminiscent of the fingering reported in reference [25]. For straight square teeth a three-lobed jet was produced, each lobe being separated by 120° in the horizontal plane and inclined at a slight positive angle to the horizontal. When the straight teeth were replaced by rectangular teeth cut on a bias, so as to impart a small degree of swirl, a six-lobed jet was produced, the three lobes previously produced being separated by additional lobes which were inclined slightly downwards.

The particular saw-toothed configuration studied experimentally—see Figures 13 and 14—was chosen to give the same flow rate as the type C exit slot of Table 1. The sound pressure level is plotted against the jet boundary velocity in Figure 5 for this saw-toothed configuration. It can be seen to be substantially quieter compared with the unmodified slot C. None of the power spectra obtained for this saw-toothed exit slot exhibited discrete tones. The peak frequency for the broadband noise was not significantly changed by fitting a saw-toothed exit slot. The microphone signal obtained by continuously increasing the stagnation pressure is shown in Figure 16. Comparison with Figures 6(a) and 6(b) shows that Figure 16 is much more similar to the signal corresponding to the unstepped model than to the one fitted with a step. There is no indication of discrete tones or flow breakaway. Thus on the model tests the saw-toothed exit slot is a very effective technique for noise suppression. One was unable to test its effect on breakaway completely, but certainly there was no sign of breakaway occurring at the highest stagnation pressure attainable with the experimental facility (i.e., $p_0 = 7{\cdot}6$ bar).

Some preliminary tests [26] in the field were carried out on a full-size Indair 33 waste gas flare. The concept was implemented rather crudely in that a fairly thick saw-toothed metal sleeve was attached around the existing exit slot. Four different sleeve geometries were tested. One sleeve appeared to interfere in an undesirable way with the Coanda effect. Another was designed for comparison with a full-size exit slot of 10 mm and it was not possible to obtain reliable control data for the unmodified flare in this case. The two

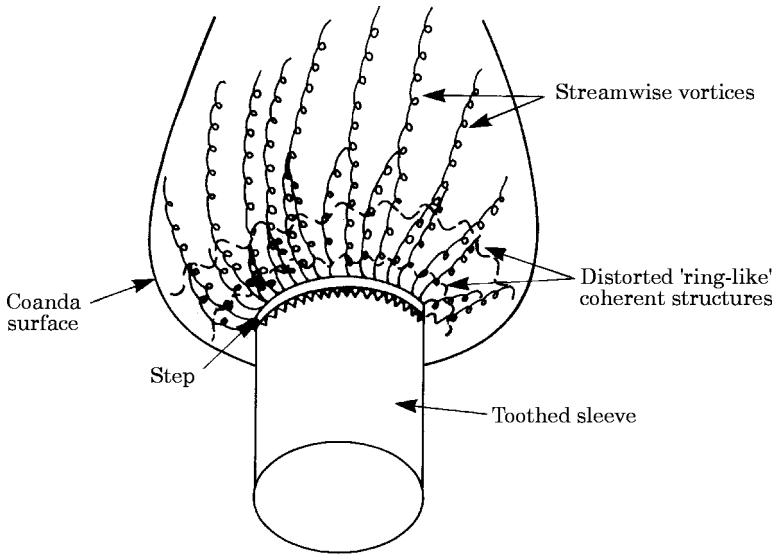

Figure 15. Schematic sketch showing the effect of streamwise vortices on the coherent structures in the region near the exit slot.

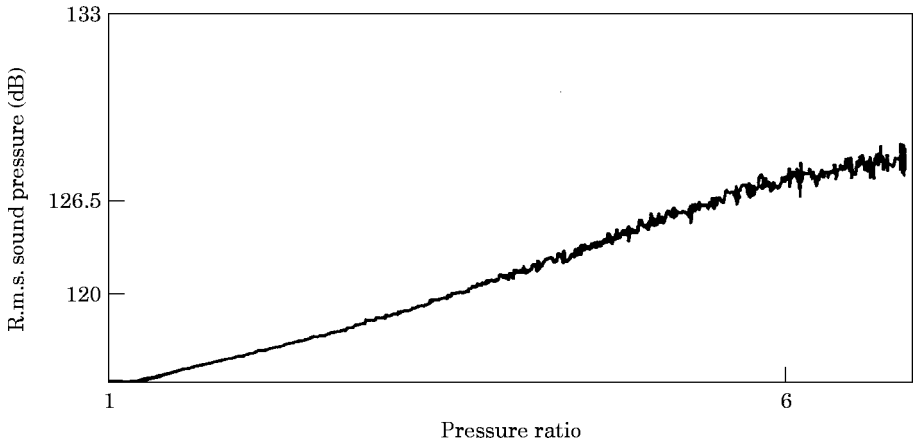

Figure 16. R.m.s. sound pressure level plotted against pressure ratio for a saw-toothed exit slot with a 2 mm step.

geometries shown in Figure 17 were designed for comparison with a full-size exit slot of 5 mm. Sound levels were measured in the field by using a hand-held Brüel & Kjaer Type 2203 precision sound level meter with a 1/2 in Type 4133 microphone. The data are plotted in Figure 17. The error bars displayed in Figure 17 are an indication of the fluctuations in the readings obtained when using the sound-level meter. These fluctuations result from the large-scale fluctuations and intermittency observed in the combustion process. It can be seen that noise reductions were obtained for both saw-toothed sleeves with about 10 dB(A) reduction when using sleeve A. The combustion process was also significantly modified by the use of the saw-toothed sleeve. The authors' subjective observation by eye and ear was that with the saw-toothed sleeve fitted, the combustion process was less intermittent and the large-scale fluctuations were significantly reduced in size. This is also

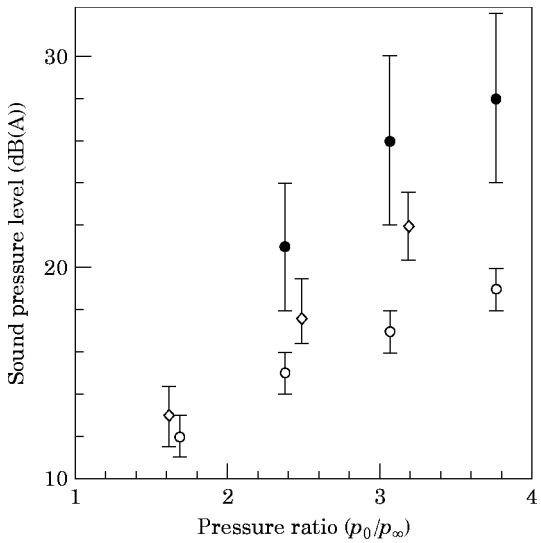

Figure 17. Sound level data from field measurements on full scale unmodified flares and those with saw-toothed sleeves. ●, 5 mm slot width (unmodified flare); ○, toothed sleeve with a triangular tooth (base = height = 100 mm); ◇, toothed sleeve (base = 200 mm, height = 100 mm). The vertical bar lines indicate the extent of the fluctuations.

evidenced by the reduction in the size of the error bars plotted in Figure 17 for the saw-toothed exit slots as compared with the unmodified flare. Presumably, this is further support for the present hypothesis that the saw-toothed exit slot reduces the scale of the coherent structures in the turbulent flow.

4. CONCLUSIONS

An investigation of the effect of flow-control devices on the flow field and aeroacoustics of a high-speed Coanda device has been described. In section 2 of the paper the effects of incorporating a step between the annular exit slot and the Coanda surface were considered. The step is incorporated to ensure that the breakaway pressure is raised to a level well above the maximum operating pressure. The following main points emerged from the present investigation of a model Coanda device fitted with a step.

(i) A base-flow region is formed immediately downstream of the step. This results in a substantial alteration to the flow field near the exit slot. In particular, a lip shock is generated which emanates from the upper edge of the exit slot at the step; but the lip shock found with the unstepped Coanda model which emanates from the lower edge of the exit slot is eliminated. In the unmodified Coanda flow this latter type of lip shock appears to generate a separation bubble when it is incident on the Coanda surface. The separation bubble grows in size as the stagnation pressure rises and ultimately causes breakaway to occur. Thus its elimination may explain why the step has a favourable effect on breakaway.

(ii) The presence of the step promotes the generation of discrete tones. There appear to be two groups of such tones. Group A occurs at relatively low stagnation pressures and for a fixed geometry the dominant frequency appears to be approximately invariant with stagnation pressure. Group B occurs at relatively high pressures and can occur in up to three separate stages. In each stage the tone first appears at a high frequency with the dominant frequency falling steeply as stagnation pressure rises. The group B discrete tones were also observed in the unmodified Coanda flows and a theoretical model was proposed in [1] to explain how they were generated.

(iii) A theoretical model is proposed to explain how the group A tones were generated. It is suggested that a self-generated feedback loop is set up whereby wave-like coherent structures propagate along the shear layer bounding the base-flow region behind the step, causing periodic inflow and outflow to occur in the reattachment zone. This would generate an acoustic source which would radiate back to the exit slot within the subsonic base-flow region. The approximate predictions obtained with this model seem to agree reasonably well with experimental observations.

Section 3 of the paper is devoted to an investigation of the effects of replacing the annular exit slot with a saw-toothed one. This modification was proposed for the purposes of noise reduction. Both model and full-scale tests are reported. The main points to emerge are:

(iv) It appears that the saw-toothed arrangement generates streamwise vortices which disrupt the coherent structures, reducing their scale and weakening the shock-cell structure. They also lead to enhanced entrainment. Discrete tones are completely eliminated with a saw-toothed exit slot, leading to much quieter flows.

(v) Some preliminary full-scale tests were carried out with saw-toothed exit slots fitted. Up to a 10 dB(A) reduction in sound pressure level was measured.

ACKNOWLEDGMENTS

The work described in this paper was undertaken as part of a research programme supported by the BP Research Centre, Kaldair Ltd. and the SERC. Much of the work

was carried out while Dr. Smith was in receipt of an SERC CASE research studentship sponsored by the BP Research Centre.

REFERENCES

1. P. W. Carpenter and P. N. Green 1997 *Journal of Sound and Vibration* **208,** 777–801. The aeroacoustics and aerodynamics of high-speed Coanda devices, Part 1: conventional arrangement of exit nozzle and surface.
2. D. H. Desty 1983 *Proceedings of the Institution of Mechanical Engineers* **197A**, 159–170. No smoke with fire.
3. D. H. Desty, J. C. Boden and R. E. Witheridge 1978 in *Proceedings of the* 85*th National Meeting of the American Institute of Chemical Engineering*, *Philadelphia*, *U.S.A*. The origination, development and application of novel premixed flare burners employing the Coanda effect.
4. B. G. Jenkins, F. D. Moles, D. H. Desty, J. C. Boden and G. Pratley 1980 *Energy Technology Conference and Exhibition*, *New Orleans*, *ASME Paper* 80-*Pet*-86. The aerodynamic modelling of flares.
5. N. Fricker, R. H. Cullender, K. O'Brien and J. A. Sutton 1986 in *Proceedings of the International Gas Research Conference*, *Toronto*, *Canada* (T. L. Cramer, editor), 989–1003. Rockville MD: Government Institutes Inc. Coanda jet pumps—Facts and fallacies.
6. C. Parsons† 1988 *Ph.D. Thesis*, *University of Exeter*, *England*. An experimental and theoretical study of the aeroacoustics of external-Coanda flares.
7. P. W. Carpenter, D. W. Bridson and P. N. Green 1986 *American Institute of Aeronautics and Astronautics* 10*th Aeroacoustics Conference*, *Seattle*, *Paper AIAA*-86-1865. Features of discrete tones generated by jet flows over Coanda surfaces.
8. D. R. Chapman 1950 *NACA Technical Note* 2137. An analysis of base pressure at supersonic velocities and comparison with experiments.
9. H. H. Korst 1956 *Journal of Applied Mechanics* **23**, 593–600. A theory for base pressures in transonic and supersonic flow.
10. D. G. Gregory-Smith and P. Senior 1994 *International Journal of Heat and Fluid Flow* **15**, 291–298. The effects of base steps and axisymmetry on supersonic jets over Coanda surfaces.
11. A. Powell 1953 *Journal of the Acoustical Society of America* **25**, 385–389. The noise of choked jets.
12. A. Powell 1953 *Aeronautical Quarterly* **4**, 103–122. On the noise emanating from a two-dimensional jet above the critical pressure.
13. J. E. Rossiter 1966 *Aeronautical Research Council*, *R & M* 3438. Wind tunnel experiments in the flow over rectangular cavities at subsonic and transonic speeds.
14. H. H. Heller, G. Holmes and E. E. Covert 1971 *Journal of Sound and Vibration* **18**, 545–553. Flow induced pressure oscillations in shallow cavities.
15. A. J. Bilanin and E. E. Covert 1973 *American Institute of Aeronautics and Astronautics Journal* **11**, 347–351. Estimation of possible excitation frequencies for shallow rectangular cavities.
16. D. W. Bogdanoff 1983 *American Institute of Aeronautics and Astronautics Journal* **21**, 926–927. Compressibility effects in turbulent shear layers.
17. D. Papamoschou and A. Roshko 1988 *Journal of Fluid Mechanics* **197**, 453–477. The compressible turbulent shear layer: an experimental study.
18. D. Papamoschou 1991 *American Institute of Aeronautics and Astronautics Journal* **29**, 680–681. Structure of the compressible turbulent shear layer.
19. S. Martens, K. K. Kinzie and D. K. McLaughlin 1994 *American Institute of Aeronautics and Astronautics Journal* **32**, 1633–1639. Measurements of Kelvin–Helmholtz instabilities in a supersonic shear layer.
20. P. W. Carpenter, N. P. Simpson and D. W. Bridson 1987 *Centre for Geophysical and Industrial Fluid Dynamics*, *University of Exeter*, *Technical Note* 87/1. Recent work on the aeroacoustics of the Indair flare.
21. H. K. Tanna 1977 *Journal of Sound and Vibration* **50**, 429–444. An experimental study of jet noise, part II: shock associated noise.
22. K. K. Ahuja and W. H. Brown 1989 *American Institute of Aeronautics and Astronautics Paper* 90-0994. Shear flow control by mechanical tabs.

† Please note that this is Dr. C. Smith's thesis published under her maiden name.

23. K. K. Ahuja, J. P. Manes, K. C. Massey and A. B. Calloway 1990 *American Institute of Aeronautics and Astronautics Paper* 90-3982. An evaluation of various concepts of reducing supersonic jet noise.
24. M. Samimy, K. B. M. Q. Zaman and M. F. Reeder 1993 *American Institute of Aeronautics and Astronautics Journal* **31**, 609–619. Effect of tabs on the flow and noise field of an axisymmetric jet.
25. K. B. M. Q. Zaman, M. F. Reeder and M. Samimy 1994 *Physics of Fluids* **6**, 778–793. Control of an axisymmetric jet using vortex generators.
26. P. W. Carpenter 1988 *Centre for Geophysical and Industrial Fluid Dynamics*, *University of Exeter*, *Technical Note* 88/1. Full-scale tests on flares fitted with the saw-toothed sleeve.